JOURNAL OF CATALYSIS 119, 146–160 (1989)

Sintering of Platinum-Black in Hydrogen: Morphology and Catalytic Activity

ZOLTÁN PAÁL, HELGA ZIMMER, JOHN R. GÜNTER,* ROBERT SCHLÖGL,† AND MARTIN MUHLER†

*Institute of Isotopes of the Hungarian Academy of Sciences, P.O. Box 77, H-1525 Budapest, Hungary, *Institute for Inorganic Chemistry, University of Zürich, Winterthurerstrasse 190, CH-8057 Zürich, Switzerland, and †Fritz-Haber-Institut der Max-Planck-Gesellschaft, Faradayweg 4-6, 1000 Berlin 33, Federal Republic of Germany*

Received October 14, 1988; revised May 20, 1989

Pt-black (Pt-473 and Pt-633) reduced in aqueous solution with HCHO was sintered at 473 and 633 K in hydrogen. Electron micrographs show a considerable sintering, especially at 633 K. High-resolution EM indicates the presence of agglomerates of rounded crystals; lattice fringes are also seen. Samples sintered at different temperatures show identical catalytic activity in ring opening and aromatization of alkylcyclopentanes; their activity was also similar in bond-shift isomerization of heptane isomers. On the other hand, aromatization, hydrogenolysis, and C_5-cyclic isomerization were more rapid on Pt-473, while C_5-cyclization was more rapid on Pt-633. These effects are discussed in terms of various active sites for these skeletal reactions and their abundance on two samples which have different morphology, hence different hydrogen retention ability; also the chemical state of their carbon impurity may be different.

INTRODUCTION

There has been much debate over the geometry of active sites of Pt catalysts at the atomic level. Skeletal reactions of various model hydrocarbons on well-defined single-crystal faces (*1–5*) contributed much to the elucidation of this problem. Faces with hexagonal symmetry [flat, stepped, and kinked (111) type planes] definitely favor aromatization of *n*-hexane (*2*); no such structure-sensitivity was reported for methylcyclopentane reactions (*3*). Five-coordinated, so-called B_5-sites were claimed to possess enhanced activity in hydrogenolysis and bond-shift isomerization reactions (*5*).

Single-crystal faces may contain various amounts of impurities. Pt single crystals showed nonnegligible activities in *n*-alkane reactions in the presence of even two to three times as much (rather stable) surface carbon as surface Pt (*1*). Garin *et al.* (*4*) found that the carbonaceous overlayer could be removed relatively easily.

In addition to the mere presence of such overlayers which create "Pt–C" active sites instead of (or in addition to) pure Pt sites, restructuring of Pt surfaces can be induced even by trace impurities, as discussed by Dauscher *et al.* (*5*). Of the additives inducing restructuring, the importance of hydrogen should be stressed. This was found to be able to induce step restructuring in Pt single crystals (*6*) as well as a dramatic sintering of high-surface freshly reduced Pt-black catalysts (*7*).

There is much speculation as to how to correlate single-crystal results with those obtained over dispersed catalysts. Even unsupported metals such as Pt-black may contain considerable amounts of impurities like silicon (*8*), carbon, and oxygen (*9–11*). Sintering during the first heat treatment is facilitated by penetration of hydrogen into subsurface layers (*7, 12*); that this hydrogen may not be removed from Pt-black by customary treatment (such as regeneration with oxygen) has been shown by tritium labeling experiments (*13*). This hydrogen, sit-

0021-9517/89 $3.00

uated partly in subsurface layers, can interact with hydrocarbon reactants (*13*) as can hydrogen attached to carbonaceous overlayers (*1*). Thus, a sintered Pt-black catalyst can be regarded as a "Pt–C–H" system exposing clean surface fractions as well as surfaces covered with carbon of varying degree of polymerization. The model we proposed for this catalyst (*11*) was not far from that postulated by Davis *et al.* (*1*) for single crystals.

A Pt-black sample (presintered in hydrogen at 633 K) showed selectivities in *n*-hexane reactions similar to single-crystal faces with (111) type of symmetry (*14*) under similar hydrogen pressures. As a function of hydrogen pressure, maxima were found for yields of various skeletal reactions of alkanes (*14–17*). Ring-opening yields of cycloalkanes increased very markedly with increasing hydrogen pressure, $p(H_2)$ (*18*), as did the selectivity of ring opening, i.e., the reactivity of bonds in positions more removed from the substituent (*15*).

Presintering of Pt-black in hydrogen at different temperatures produced various crystallite sizes, as demonstrated by electron microscopy, EM (*7, 8*), and XRD (*12*). The surface composition and also the chemical state of the surface impurity was influenced by the sintering temperature (*9–11*). Although even high-resolution electron microscopy is not yet able to distinguish surface structures at the atomic level, it may reveal crystal shapes and lattice fringe images of model or real catalysts under various conditions (*19–23*). In this way, one may estimate the sizes of individual crystallites and the crystal faces likely to be exposed. For example, the lattice fringes indicated that a Pt particle on an alumina support represented a single crystal in spite of its complex shape (*24*); a low-resolution transmission electron micrograph could have indicated an agglomerate of smaller crystallites. The crystal shapes observed were compared with catalytic properties (*19*).

In the present study, transmission electron microscopy of samples presintered at 473 and 633 K will be reported together with their activity in test reactions of several "archetypal" (*25*) C_7-alkanes and cycloalkanes. Results concerning *n*-hexane and methylcyclopentane are reported elsewhere (*26a*).

Preliminary data on surface analysis by XPS and AES of our catalysts after use will be used to decide whether visible morphology or different surface composition is the main reason why different catalytic properties are observed. Detailed data will be published later (*26b*).

EXPERIMENTAL

Catalysts. Pt-black reduced in aqueous medium from H_2PtCl_6 by HCHO in the presence of excess KOH between 273 and 278 K (*16*) was presintered according to a "standard thermal cycle" (STC) as defined in Ref. (*7*). The temperatures were 473 and 633 K; the samples are denoted by Pt-473 and Pt-633, respectively.

Electron microscopy. The Pt samples were suspended in bidistilled water by ultrasonic treatment (1 MHz for 3 min) and dried onto holey carbon films supported on standard copper specimen grids. Electron micrographs were recorded by means of a transmission electron microscope JEM 200-CX (JEOL Ltd., Japan) equipped with a top-entry specimen stage and ultrahigh-resolution objective pole piece, operated at 200 kV, at maximum magnifications of 550,000. Further enlargement was done photographically. Additional measurements were also carried out with a Zeiss EF instrument.

Catalytic measurements. A static-circulation apparatus was used at $T = 603$ K under constant hydrocarbon pressure of 1.23 kPa and hydrogen pressure varying between 4 and 60 kPa (*14, 16*). Sampling was done after 5 min of reaction time. The mass of catalysts used was 100 mg; the number of surface Pt atoms on these 100-mg samples was calculated from N_2/BET specific surfaces. The values per 100 mg are 4.92×10^{18} for Pt-473 and 2.25×10^{18} for Pt-633. Catalytic activities were expressed as turnover

numbers (TON), molecules reacted (or produced) per surface Pt atom per second.

Materials: Hydrocarbons of 99 to 99.9% purity were used. *n*-Alkanes have been described in Ref. (*14*), cycloalkanes in Ref. (*18*).

RESULTS

Electron microscopy. Fresh Pt-black is a very finely dispersed material; its average crystallite size can be estimated to be between 5 and 12 nm (Fig. 1A). Sintering at 473 K produces a material with crystallite sizes of 20–50 nm (Fig. 1B) whereas the crystallite size of Pt-633 is around 100 nm, higher than that observed earlier (*7, 8*). Rounded crystals of sintered Pt are observable (Fig. 1C).

The high-resolution electron micrograph of fresh, unsintered Pt-black shows agglomerates of rounded crystals (Fig. 2A). Lattice fringes are clearly visible. Some moiré patterns indicate that one crystallite may be found above another; the presence of twins as seen in supported Pt samples (*20, 22*) is not excluded. The absence of angular crystal shapes without large flat planes exposed may indicate surface contamination, as suggested by Wang *et al.* (*27*). This is in agreement with surface analysis data. The electron diffraction pattern corresponds to a very finely dispersed structure. Sintering at 473 K produces crystals at the limit of transparency in the electron beam (Fig. 2B). Lattice fringes indicate the presence of at least two single crystals in the picture and also two contact areas between individual crystallites can be clearly distinguished. The amorphous patch at the extreme right of the figure may correspond to a three-dimensional, probably amorphous, carbonaceous deposit (*28*). The curved character of the crystal borderline indicates the appearance of various steps. The electron diffractograms also suggest a distinct increase in crystallite size. Pt-633 was not transparent, thus no high-resolution micrographs could be taken. The curved character of the exposed surface can be judged from the low-magnification picture (Fig. 1C). This sample should contain more surface carbon (*9–11*), which is probably polymeric but not graphitic (*8, 9*).

Catalytic measurements. Formation of individual product classes has been plotted as a function of the hydrogen pressure. Figures 3 to 6 show the turnover numbers of hydrogenolysis, C_5-cyclization, and isomerization from various alkanes. The two catalysts show dramatic differences in the yields of *hydrogenolysis* (Fig. 3), Pt-433 being more active by up to one order of magnitude. Also the character of hydrogen pressure response is totally different. Pt-633 shows the expected (*14–17*) maximum curves whereas the increase of $p(H_2)$ monotonically increases all yields over Pt-473. Also reactant hydrocarbon structure effects are present: while a smaller difference is seen for 3-methylhexane, dramatic variation of yields appears with 3,3-dimethylpentane with a quaternary carbon atom.

The yields of *C_5-cyclic products* are comparable on the two samples (Fig. 4). Here the activity order is reversed, Pt-473 being less active. The order of reactivities of individual reactant alkanes corresponds to that described previously (*29*). Both catalysts may produce maxima although Pt-473 produces less pronounced ones and in fewer cases.

Figure 5 depicts the formation of *skeletal isomers* that could be formed by a C_5-cyclic pathway (*30*). The shape of the hydrogen dependences is similar to those seen in C_5-cyclization. Previously this similarity was taken as evidence for the relation between C_5-cyclization and isomerization. The C_5-cyclic pathway in skeletal isomerization prevails in most cases (*15, 30, 31*), so we do not have reason to doubt its importance even over Pt-473 where the hydrogen dependences are profoundly dissimilar. The sequence of reactivities of different hydrocarbons is the same over both catalysts. Monotonically increasing yields of *bond-shift isomerization* were observed on Pt-633 previously (*14*) and these occurred over both catalyst samples here, the activity of the samples being nearly the same (Fig. 6).

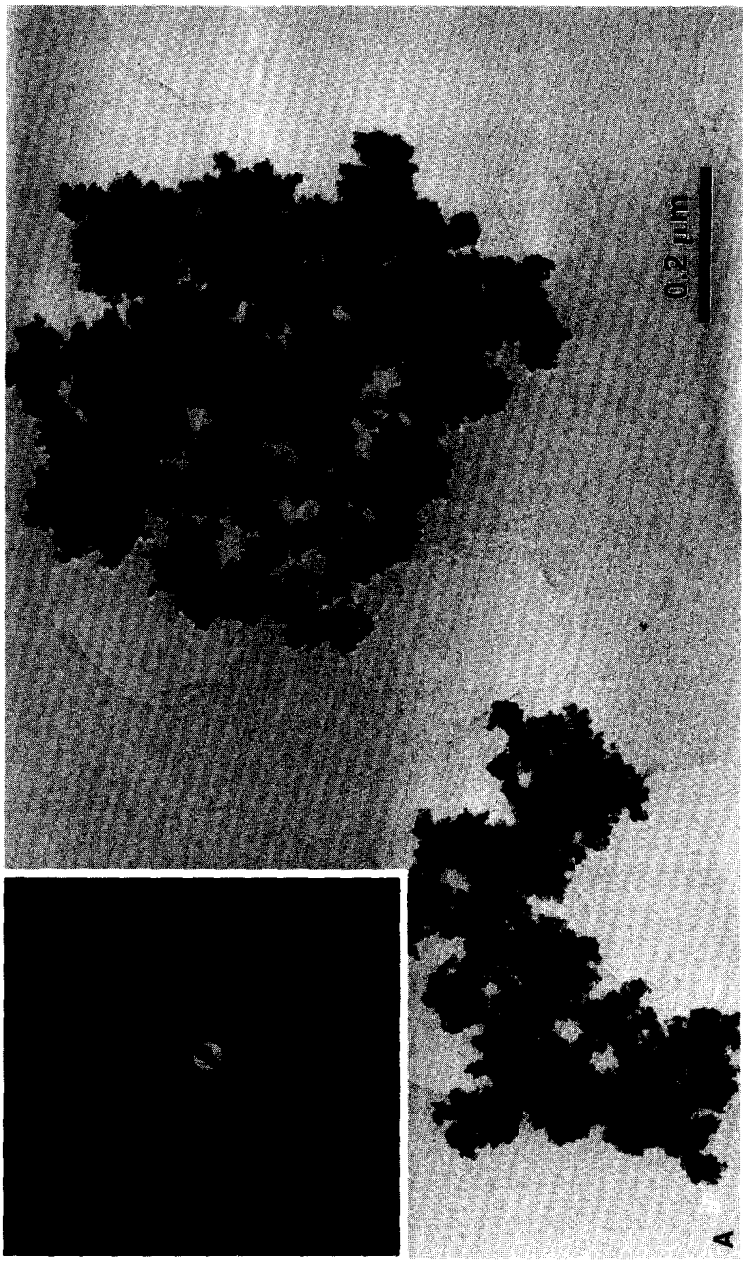

FIG. 1. Transmission electron micrographs of Pt-black. (A) Aggregates of finely divided fresh Pt-black. Inset: selected area electron diffraction (SAED) pattern. (B) An aggregate of Pt-473 with increased particle size. Inset: SAED pattern. (C) Rounded sintered Pt-633 particles, opaque to electrons.

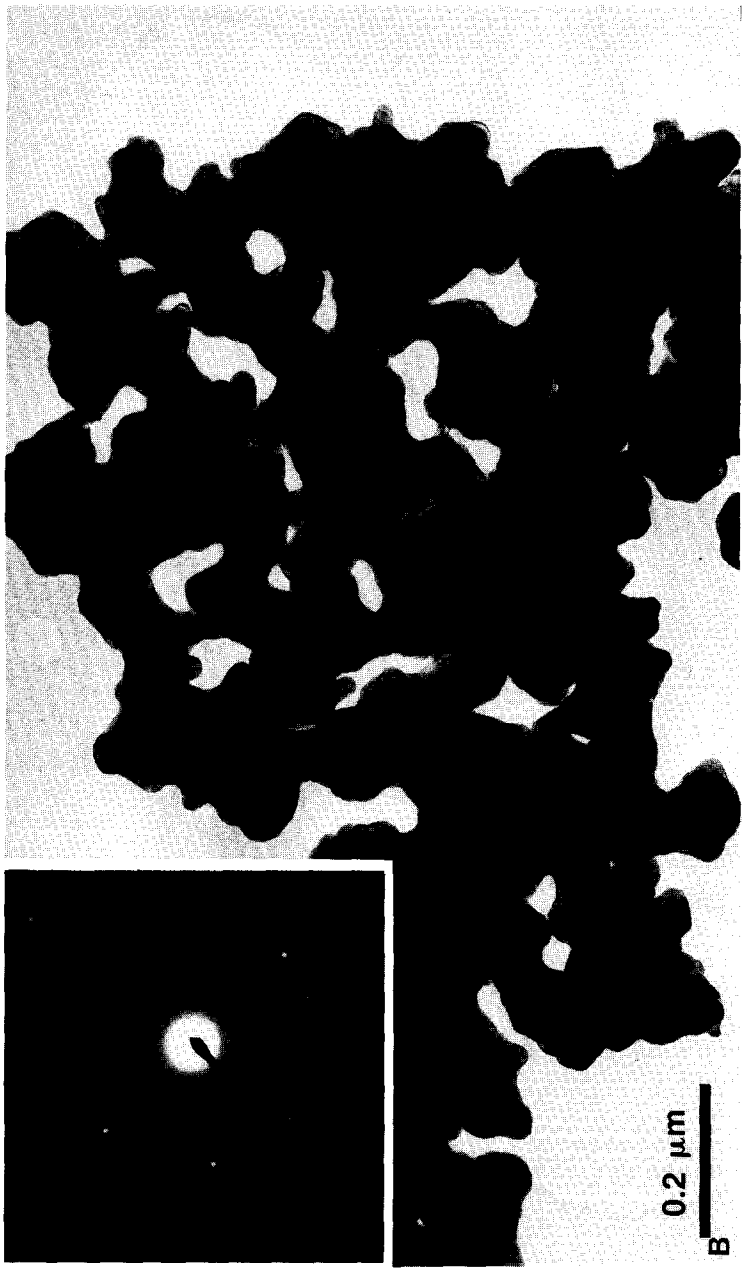

FIG. 1—*Continued*

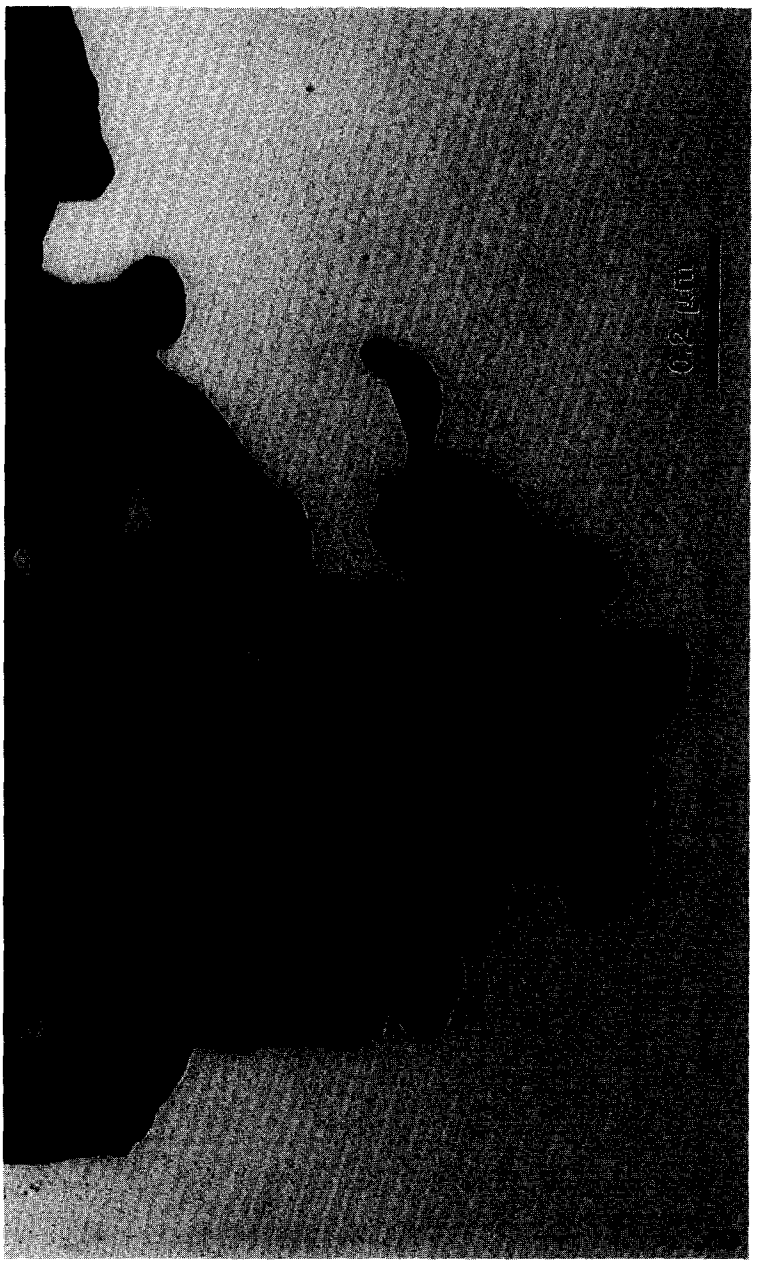

FIG. 1—*Continued*

FIG. 2. High-resolution transmission electron micrographs of Pt-black. (A) Fresh sample: lattice fringes and moiré patterns are clearly visible. (B) Pt-473. Lattice fringes extend over large areas up to 50 nm. Note contact areas between crystallites and an amorphous patch at the right-hand edge of the figure.

FIG. 2—*Continued*

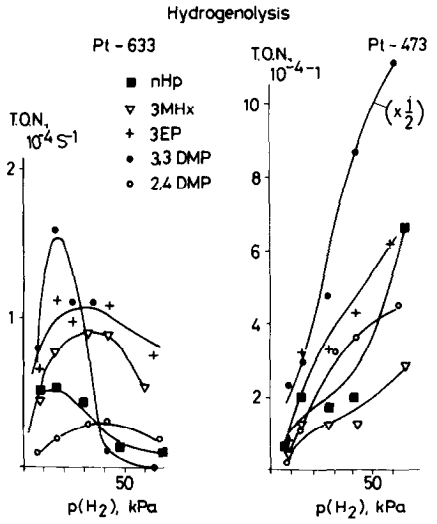

FIG. 3. Hydrogenolysis yields of five heptane isomers on Pt-633 and Pt-473 as a function of hydrogen pressure (expressed as turnover numbers, TON, 10^{-3} molecule reacted per surface Pt per second).

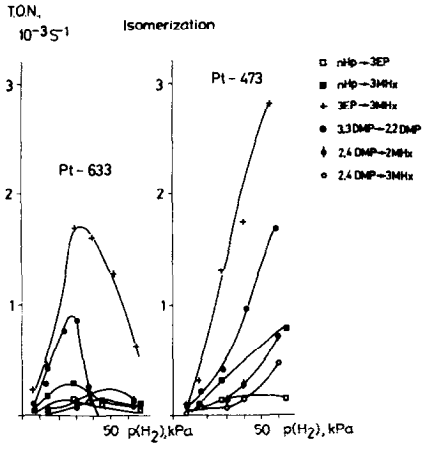

FIG. 5. Turnover numbers of individual isomers from various heptane isomers.

Aromatization of alkanes and cycloalkanes are shown together in Figs. 7 and 8. Maximum curves for Pt-633 and monotonic increase or minimum curves are seen with Pt-473, the overall activity being in the same range. A dramatic increase manifests itself in aromatization of *n*-heptane under elevated $p(H_2)$ and also in the reaction of 3,3-dimethylpentane.

Hydrocarbon reactant structure sensitivity is seen in the *selectivities* of three selected alkanes (Table 1). The quaternary structure favors hydrogenolysis; the selectivity of this reaction is always higher on Pt-633 although absolute rates are higher on Pt-473 (Fig. 3).

The pattern of hydrogenolysis, expressed as ω-values as defined by Leclercq *et al.* (*32*), is different and shows different hydrogen responses on Pt-473 and Pt-633. Data for *n*-heptane are shown as an example in Table 2.

Cyclopentanes produced much higher aromatic yields than alkanes; here the two

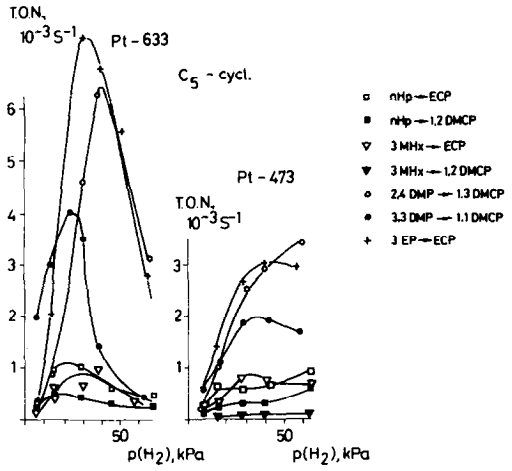

FIG. 4. Turnover numbers of C_5-cyclic products from various heptane isomers.

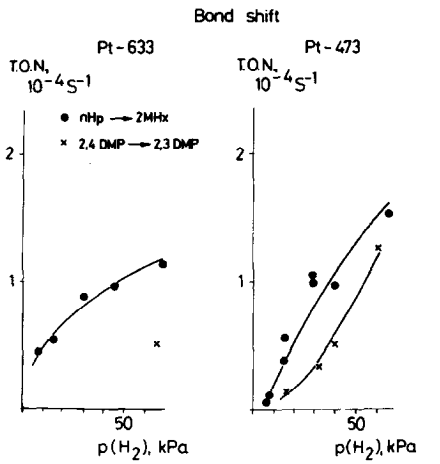

FIG. 6. Turnover number of isomers which could only have formed via bond shift.

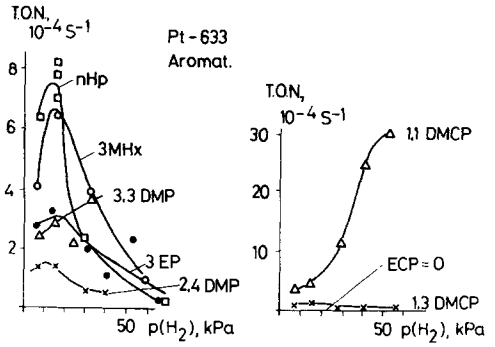

FIG. 7. Aromatization of C_7-alkanes and -cyclopentanes over Pt-633.

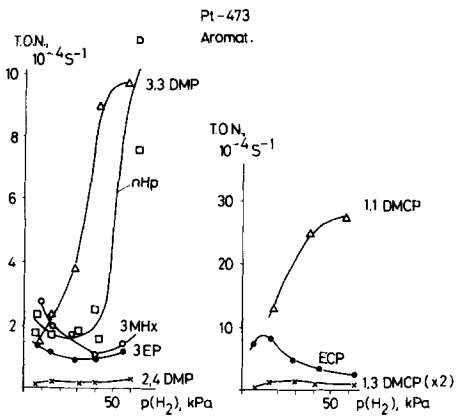

FIG. 8. Aromatization of C_7-alkanes and -cyclopentanes over Pt-473.

samples had nearly identical activities. *Ring opening* of cycloalkanes is usually their most important reaction (*18, 30, 31*) and this is the case over both of our samples, too. Figure 9 also compares cyclopentane and methylcyclopentane, the reactivity of which is higher (*18*) than that of most C_7-cycloalkanes (except, again, for 1,1-dimethylcyclopentane). The turnover number of this type of reaction is highest and the TON difference between the two samples is very small; where there are differences, Pt-633 is more active.

TABLE 1

Selectivity of Transformations of Selected Alkanes over Pt-473 and Pt-633 Catalysts

Hydrocarbon reactant	Selectivity (%)						Isomer $\frac{}{C_5\text{-cyclic}}$
	$p(H_2)$ (kPa)	$<C_7$	Iso.	C_5-cycl.	Olef.	Arom.	
A. Pt-633							
n-Heptane	7.5	24.7	14.4	27.5	—	31.3	0.52
	32.0	15.6	19.1	54.3	—	9.2	0.35
	73.0	8.5	19.9	63.8	—	4.8	0.31
3-Ethylpentane	6.6	52.3	7.8	13.3	17.1	9.4	0.59
	33.5	26.7	13.1	55.1	3.6	5.2	0.24
	70.0	17.0	14.5	62.7	5.2	0.6	0.23
3,3-Dimethylpentane	6.8	50.5	1.7	39.7	2.4	5.6	0.04
	34.0	35.6	12.0	47.3	—	5.2	0.25
	43.0	28.0	8.4	63.6	—	—	0.13
	68.0	—	—	100	—	—	—
B. Pt-473							
n-Heptane	7.0	2.0	30.7	32.0	2.6	32.7	0.96
	30.5	8.0	37.7	49.4	—	5.0	0.76
	70.0	11.0	34.0	34.2	—	20.4	0.99
3-Ethylpentane	8.5	4.3	4.5	34.6	48.9	7.6	0.13
	30.5	6.8	27.0	55.0	9.3	1.8	0.49
	61.0	8.2	37.5	39.3	13.4	1.6	0.95
3,3-Dimethylpentane	9.2	35.7	4.8	46.3	2.3	11.5	0.10
	31.5	26.4	10.9	50.3	1.6	10.3	0.22
	45.0	31.5	17.0	34.3	1.0	16.1	0.50
	64.0	40.2	29.9	30.6	1.3	17.1	0.98

TABLE 2

Hydrogenolysis Pattern of *n*-Heptane[a]

Catalyst: $p(H_2)$ (kPa)	Pt-473			Pt-633[b]		
	7	30.5	70	7.5	32	73
ω_1 (C_1–C_2)	0.4	0.9	1.1	0.2	0.7	0.8
ω_2 (C_2–C_3)	1.5	0.9	0.95	2.3	1.3	0.8
ω_3 (C_3–C_4)	1.1	1.2	0.95	0.5	0.9	1.4

[a] Defined as ω = actual rate of rupture/random rate of rupture for each C–C bond (*32*).

[b] Data taken from Ref. (*33*).

It is worth mentioning the much disputed positional selectivity of C_5-ring opening. Here particle size effects were reported (*30*); the increase of hydrogen pressure accelerated ring opening in positions farther from the side alkyl group, this hydrogen effect being superimposed on the particle size effect (*15*). Table 3 reveals that a less marked hydrogen dependence is seen with Pt-473.

Surface analysis. Table 4 summarizes new XPS and AES data together with previous XPS results (*10*) where the possible

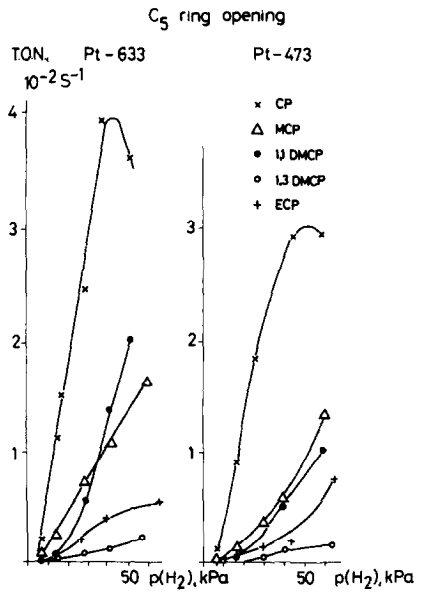

FIG. 9. Ring-opening yields of cyclopentane and various alkylcyclopentanes as a function of the hydrogen pressure over Pt-473 and Pt-633.

TABLE 3

Ring Opening Selectivities over Various Pt-Black Samples

Catalyst: $p(H_2)$ (kPa)[a]	Pt-473			Pt-633		
	7	32	70	7	32	70
Reactant: methylcyclopentane[b]						
b/*a*	3.6	4.0	4.3	0.26	2.9	6.6
b/*c*	1.8	2.0	2.2	1.5	1.3	2.1
Reactant: ethylcyclopentane[c]						
b/*a*	1.4	3.2	2.1	1.3	2.5	3.9
b/*c*	5.0	3.9	2.5	3.6	2.7	2.2

[a] ±10%.

[b] Position *a*: *n*-hexane; *b*: 2-methylpentane; *c*: 3-methylpentane.

[c] Position *a*: *n*-heptane; *b*: 3-methylhexane; *c*: 3-ethylpentane.

contamination of the surface with hydrocarbon residual gases was first mentioned. Experimental details are included. The new

TABLE 4

Surface Composition of Pt-Black Samples[a]

Sample	Method	Surface composition (atom %)				
		Pt	O	C	K	Si
Pt-473						
STC[b]	XPS[c]	19	22	59	—	—
	XPS	38	26	34	2	—
	AES	76	4	16	3	1
Used[b]	XPS	31	23	45	1	—
	AES	76	1	19	3	1
Pt-633						
STC[b]	XPS[c]	13	24	63	—	—
Used[b]	XPS	29	21	49	1	—
	AES	71.5	3	22	3	0.5

[a] Apparatus and conditions: Leybold LHS-12, Mg$K\alpha$ radiation: XPS, 12 kV, 20 mA, pass energy 50 eV; AES, 5000 V, $E/\Delta E$ = 4; hemispherical analyzer EA 11. Data processing: Leybold DS 100 software (background fit and integration for XPS, smoothing and differentiation for AES).

[b] STC signifies sintered sample (*7*). "Used" signifies sample removed from the reactor after lengthy use at $T \leq 663$ K. Samples were stored in air in both cases for several months.

[c] XPS data from Ref. (*10*).

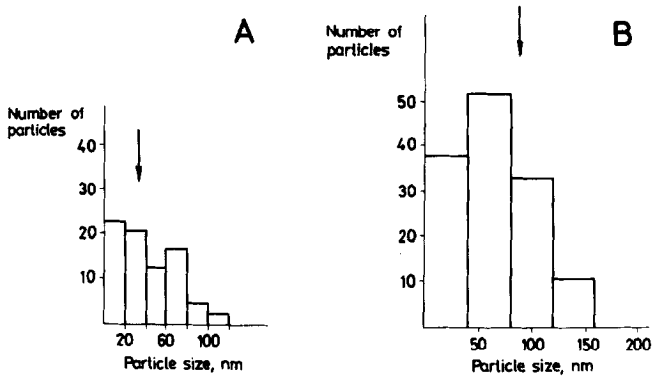

FIG. 10. Particle size distribution of Pt-473 (A) and Pt-633 (B). The arrows show the average particle size determined by X-ray line broadening. Another batch of catalysts was used for this measurement which was carried out by a Zeiss EF instrument. Thanks are due to Dr. E. Czárán and Ms. G. Erdei for this determination.

XPS data show more Pt and less C on the surface with almost identical amounts of O, indicating that the surface C content was previously overestimated. The presence of minor amounts of K (*11*) and Si (*8*) has been confirmed. The more surface-sensitive AES shows a much cleaner Pt surface, indicating that many of the impurities are situated below the surface, either dispersed along the imperfections of the bulk metal as indicated in the model in Ref. (*11*) or present on the internal surfaces of the microscopic voids seen in Fig. 1, which are significant with a loose powder sample. Potassium from the preparation process, on the other hand, tends to accumulate on the surface.

DISCUSSION

The activity of the catalysts in question is determined by the abundance of active sites which, in turn, is determined by the original structure and purity of the catalysts.

Different abundances of various surface arrangements arise with crystallites smaller than about 4–5 nm (*34*). The electron micrographs (Figs. 1 and 2) make it obvious that they are out of the question in our case: the smallest particle seen is about 5 × 10 nm (Fig. 2A) and these particles coalesce into larger ones during sintering. Nevertheless, it is worth checking this with particle statistics (considering also the difficulties mentioned in the Introduction). This indicates (Fig. 10) that, indeed, most particles have dimensions well above the range where particle size effects (*30, 31*) could be expected in catalytic properties.

The high-resolution electron micrographs also show that the surface of our samples cannot be approximated by a single (low- or high-index) crystal plane. This must be true also for Pt-633 where no such micrograph was available. The reactions may "select" their optimum active sites, their availability depending on (i) surface morphology, (ii) surface blocking by impurities, and (iii) the composition of the site, such as free ensembles of Pt atoms, Pt–H, Pt–C–H, etc. (*1, 14, 35–37*).

The purity of the two samples being similar, we are inclined to explain the difference of catalytic properties in terms of *catalyst morphology* and one of its consequences, namely, a different *hydrogen retention ability* for the two samples. The abundance of surface hydrogen is controlled by hydrogen pressure in the gas phase *and* by the facility of surface–subsurface hydrogen transfer (*13, 35*). The clearly visible grain boundaries in Pt-473 as opposed to the almost molten character of Pt-633 may readily offer "gates" for hydrogen penetration inside the grains (*7*). This possibility would increase hydrogen availability whenever Pt–H ensembles are required for catalysis as

well as contribute to removal of excess hydrogen from the surface whenever a competition between H and hydrocarbon species may hinder catalysis.

Whereas the content of catalyst oxygen (which is in subsurface positions) does not change much during use, the catalyst surface becomes gradually covered with carbon. Carbon accumulation may also be possible in voids. This carbon may not be identical to individual C-atoms which can have an effect similar to that of inert alloying metals (*36*) and which may gradually accumulate from hydrocarbon reactants during catalytic runs (*37*).

The role of K in facilitating π-bonded structure on Pt was recently pointed out (*38a*). K is claimed to block eight Pt atoms (*38b*); i.e., a considerable part of the available surface could be under its influence (Table 4). However, the differences between Pt-473 and Pt-633 may not be large enough to account for K-effects as the sole cause of the different catalytic properties. Specially designed experiments are required to clarify the role of potassium.

What can be deduced regarding the possible active sites and likely surface intermediates? Let us consider first the reactions which are similar over both samples. The McKervey–Rooney–Samman mechanism of *bond-shift isomerization* (*39*) requires single metal atom sites. In that case, surface-structure insensitivity could be expected and, in fact, is found (Fig. 6). The same may be valid for the *aromatization* of cycloalkanes which is likely to proceed via a bond-shift type ring enlargement route without intermediate desorption (*40, 41*). Here the high reactivity of 1,1-dimethylcyclopentane should be pointed out. The facility of ring enlargement of quaternary structures is in agreement with predictions based upon earlier experiments (*30, 41*).

We proposed two-atom sites for *C_5-cyclic reactions, ring closure and ring opening* (*14, 18, 29*). No surface-structure sensitivity has been observed with methylcyclopentane reactions over Pt single-crystal surfaces (*3*). Obviously, ensembles of two contiguous metal atoms can be found with nearly equal probability over both samples (as well as on any single-crystal plane): ring opening takes place rapidly and with equal activity. The steeper increase of *b/a* selectivities with hydrogen pressure over Pt-633 points to a stronger competition for free sites between hydrocarbon and hydrogen. The conspicuous *b*-preference of ring opening of ethylcyclopentane may indicate that this molecule is too large for two-atom sites, especially since the ethyl side group may be attached as a 3C-complex to the surface.

Under higher $p(H_2)$, hydrogen can displace the intermediates of C_5-cyclic reactions from the surface of Pt-633; yields of both C_5-cyclics *and* isomers drop. On Pt-473 even abundant hydrogen does not prevent the formation of surface 5C species. The drop of C_5-cyclic yields on Pt-473 under higher $p(H_2)$ is due to their rapid transformation into isomers. Hence, the "hydrogen utilization" of this catalyst (last column, Table 1) (*35*) is much better. This may be partly due to the higher amount of subsurface hydrogen which, with the given catalyst morphology, can be more easily mobilized under hydrogen-rich conditions (*13*). The higher reactivity of cyclopentane in ring opening and of substituted pentanes (with five C-atoms in the main chain) in ring closure/isomerization may be in accordance with the assumption that such molecules may also react more easily on single metal atoms (*14, 18*), as proposed earlier by Finlayson *et al.* (*42*). The above picture for 3C and 5C isomerization, assuming one- and two-atom sites, respectively, is a somewhat simplified picture of that deduced from alloy studies (*43*) but is certainly not in contradiction with those conclusions.

The Anderson–Avery mechanism for *hydrogenolysis* presupposed rather large ensembles (*44*). The higher activity of Pt-473 has to be pointed out: here "H–Pt–C" ensembles seem also to possess fragmentation activity. Indeed, the presence of C-atoms in

"valley" positions was suggested for terminal C–C bond rupture (*43*). The increase of the yields together with ω_1 as a function of $p(H_2)$ over Pt-473 may point to the presence of such surface species (Table 2). At the same time, internal splitting ω_3, called "frustrated isomerization" by Gault [see Ref. (*43*), p. 176], is higher under low $p(H_2)$ over Pt-473 which has a marked isomerizing activity. Under highest $p(H_2)$ isomerization is not frustrated any more (cf. Table 2 and Fig. 5). The higher ω_3 over Pt-633 under this $p(H_2)$ may be related to the suppression of isomerization (Table 2, Fig. 5). The variation of ω_2 may be related to the C_5-unit splitting (*14*).

Carbonized catalysts showed higher fragmentation selectivities at lower overall activity (*1, 26, 45*). The same tendency seems to be effective here, too (Table 1); although the yields are low over Pt-633 under high $p(H_2)$, hydrogenolysis selectivity is higher than on Pt-473. Sárkány (*46*) argues that clean Pt surfaces should favor hydrogenolysis over nondestructive reactions; also the structure sensitivity of Pt carbonization (*47*) points to the same end. In fact, it is not excluded that two hydrogenolysis mechanisms may operate as a function of the hydrogen pressure, as found by Gudkov *et al.* for ethane (*48*). One of these hydrogenolysis mechanisms may involve single atoms (*49, 50*). However, we must exert extreme care when dealing with single-atom hydrogenolysis as our data are far from sufficient for this purpose.

We think that the different hydrogen sensitivities of aromatization and isomerization + C_5-cyclization of alkanes can be explained by different reasons. Ensembles of one to three metal atoms were suggested to be active for *aromatization* (*51*). The significance of three-atom ensembles is in agreement with the enhanced aromatization activity of single-crystal faces with hexagonal symmetry (*2*). This may be the ensemble size, the magnitude of which is already different over Pt-473 and Pt-633. Apart from its more sintered character, the more polymerized character of carbon (*9*) on the latter catalyst may also be responsible for this. Under higher $p(H_2)$ values, the Pt–H sites do not represent ensembles suitable for aromatization. The scattered carbon atoms on Pt-473 may create additional active sites "H–Pt–C" under higher $p(H_2)$ (*37*); this is why aromatization yields may jump upwards under these conditions (Fig. 8). Obviously, these sites are suited first of all for aromatization without skeletal rearrangement (*n*-heptane, 3-methylhexane). The situation is similar over supported Pt (*45*). It is not excluded that enhanced aromatization under high $p(H_2)$ involves a "direct" aromatization pathway (*52, 53*). The quaternary C-atom of 3,3-dimethylpentane (*41*) facilitates its rearrangement also to an aromatic ring as the end product (see above).

To sum up, although sintering of Pt-black at different temperatures produces crystallites of different dimensions, the variations in catalytic hydrocarbon reactions are not "true" crystallite size effects; rather, they are due to various exposed crystal planes as well as to different amounts and availability of hydrogen in subsurface layers.

ACKNOWLEDGMENTS

Helpful discussions with Professor P. Tétényi are gratefully acknowledged. The research was financially supported by Research Grant OTKA 1309 (National Foundation for Scientific Research). One of us (Z.P.) thanks Professor G. Ertl for arranging a stay in Berlin during which surface analysis could be carried out, and also the Max-Planck-Gesellschaft for financial support during this stay.

REFERENCES

1. Davis, S. M., Zaera, F., and Somorjai, G. A., *J. Catal.* **77,** 439 (1982).
2. Davis, S. M., Zaera, F., and Somorjai, G. A., *J. Catal.* **85,** 206 (1984).
3. Zaera, F., Godbey, D., and Somorjai, G. A., *J. Catal.* **101,** 73 (1986).
4. Garin, F., Aeiyach, S., Légaré, P., and Maire, G., *J. Catal.* **77,** 323 (1982).
5. Dauscher, A., Garin, F., and Maire, G., *J. Catal.* **105,** 233 (1987).
6. Maire, G., Bernhardt, P., Légaré, P., and Lindauer, G., *in* "Proceedings, 7th Vacuum Congr. and 3rd Int. Conf. on Solid Surf., Vienna, Sept.

1977" (R. Dobrozemsky *et al.*, Eds.), Vol. 1, p. 861.
7. Baird, T., Paál, Z., and Thomson, S. J., *J. Chem. Soc. Faraday Trans. 1* **69,** 50 (1973); **69,** 1237 (1973).
8. Barna, A., Barna, P. B., Tóth, L., Paál, Z., and Tétényi, P., *Appl. Surf. Sci.* **14,** 85 (1982–1983).
9. Paál, Z., Tétényi, P., Kertész, L., Szász, A., and Kojnok, J., *Appl. Surf. Sci.* **14,** 101 (1982–1983).
10. Paál, Z., Tétényi, P., Prigge, D., Wang, X. Zh., and Ertl, G., *Appl. Surf. Sci.* **14,** 307 (1982–1983).
11. Paál, Z., and Marton, D., *Appl. Surf. Sci.* **26,** 161 (1986).
12. Manninger, I., Paál, Z., and Tétényi, P., *Z. Phys. Chem. N.F.* **132,** 193 (1982); **143,** 247 (1985).
13. Paál, Z., and Thomson, S. J., *J. Catal.* **30,** 96 (1973).
14. Zimmer, H., Dobrovolszky, M., Tétényi, P., and Paál, Z., *J. Phys. Chem.* **90,** 4758 (1986).
15. Bragin, O. V., Karpinski, Z., Matusek, K., Paál, Z., and Tétényi, P., *J. Catal.* **56,** 219 (1979).
16. Zimmer, H., Paál, Z., and Tétényi, P., *Acta Chim. Acad. Sci. Hung.* **111,** 513 (1982).
17. Paál, Z., *J. Catal.* **91,** 181 (1985).
18. Zimmer, H., and Paál, Z., *J. Mol. Catal.* **51,** 261 (1989).
19. Glassl, H., Kramer, R., and Hayek, K., *J. Catal.* **63,** 167 (1980); **68,** 388 (1981); Gehrer, E., and Hayek, K., *J. Mol. Catal.* **39,** 293 (1987).
20. Smith, D. J., White, D., Baird, T., and Fryer, J. R., *J. Catal.* **81,** 107 (1983).
21. White, D., Baird, T., Fryer, J. R., Freeman, L. A., and Smith, D. J., *J. Catal.* **81,** 119 (1983).
22. Harris, P. J. F., *J. Catal.* **97,** 527 (1986).
23. Sushumna, I., and Ruckenstein, E., *J. Catal.* **108,** 77 (1987).
24. Spanner, M., Baird, T., Fryer, J. R., Freeman, L. A., and Smith, D. J., *in* "EUREM '84" (Á. Csanády *et al.*, Eds.), p. 1153, 1984.
25. Foger, K., and Anderson, J. R., *J. Catal.* **64,** 448 (1980).
26. (a) Paál, Z., Zimmer, H., and Günter, J. R., *Z. Phys. Chem. N.F.*, in press; (b) Paál, Z., Xu, Xian Lun, Zhan Zhaoqi, Schlögl, R., and Muhler, M., in preparation.
27. Wang, T., Lee, C., and Schmidt, L. D., *Surf. Sci.* **163,** 181 (1985).
28. Fryer, J. R., and Paál, Z., *Carbon* **11,** 665 (1973).
29. Zimmer, H., and Paál, Z., *in* "Proceedings, 8th International Congress on Catalysis Berlin, 1984," Vol. 3, p. 417. Dechema, Frankfurt-am-Main, 1984.
30. Gault, F. G., *in* "Advances in Catalysis" (D. D. Eley, H. Pines, and Paul B. Weisz, Eds.), Vol. 30, p. 1. Academic Press, New York, 1981.
31. Maire, G., and Garin, F., *in* "Catalysis, Science and Technology" (J. R. Anderson and M. Boudart, Eds.), Vol. 6, p. 161. Springer-Verlag, Berlin/New York, 1984.
32. Leclercq, G., Leclercq, L., and Maurel, L., *J. Catal.* **50,** 87 (1977).
33. Zimmer, H., Paál, Z., and Tétényi, P., *Acta Chim. Hung.* **124,** 13 (1987).
34. van Hardeveld, R., and Hartog, F., *Surf. Sci.* **15,** 189 (1969).
35. Paál, Z., *in* "Hydrogen Effects in Catalysis" (Z. Paál and P. G. Menon, Eds.), p. 449. Dekker, New York, 1988.
36. Vogelzang, M. W., Botman, M. J. P., and Ponec, V., *Faraday Discuss Chem. Soc.* **72,** 33 (1981).
37. Sárkány, A., *J. Chem. Soc. Faraday Trans. 1* **84,** 2267 (1988).
38. (*a*) Windham, R. G., Bartram, M. E., and Koel, B. E., *J. Phys. Chem.* **92,** 2862 (1988); (*b*) Zhou, X.-L., Zhu, X.-Y., and White, J. M., *Surf. Sci.* **193,** 387 (1988).
39. McKervey, M. A., Rooney, J. J., and Samman, N. G., *J. Catal.* **30,** 330 (1973).
40. Amir-Ebrahimi, V., and Gault, F. G., *J. Chem. Soc. Faraday Trans. 1* **77,** 1813 (1981).
41. (*a*) Kane, A. F., and Clarke, J. K. A., *J. Chem. Soc. Faraday Trans. 1* **76,** 1640 (1980); (*b*) Kazansky, B. A., Liberman, A. L., Loza, G. V., and Vasina, T. V., *Dokl. Akad. Nauk SSSR* **128,** 1188 (1959).
42. Finlayson, O. E., Clarke, J. K. A., and Rooney, J. J., *J. Chem. Soc. Faraday Trans 1* **80,** 191 (1984).
43. Ponec, V., *in* "Advances in Catalysis" (D. D. Eley, H. Pines, and Paul B. Weisz, Eds.), Vol. 32, p. 149. Academic Press, New York, 1983.
44. Anderson, J. R., *in* "Advances in Catalysis" (D. D. Eley, H. Pines, and Paul B. Weisz, Eds.), Vol. 23, p. 1. Academic Press, New York, 1973.
45. Paál, Z., Zimmer, H., and Tétényi, P., *J. Mol. Catal.* **25,** 99 (1984).
46. Sárkány, A., *Catal. Today* **5,** 173 (1989).
47. Lankhorst, P. P., de Jongste, H. C., and Ponec, V., *in* "Catalyst Deactivation" (B. Delmon and G. F. Froment, Eds.), p. 43. Elsevier, Amsterdam/New York, 1980.
48. Gudkov, B. S., Guczi, L., and Tétényi, P., *J. Catal.* **74,** 207 (1982).
49. Anderson, J. B. F., Burch, R., and Cairns, J. A., *J. Catal.* **107,** 364 (1987).
50. Engstrom, J. R., Goodman, D. W., and Weinberg, W. H., *J. Amer. Chem. Soc.* **108,** 4653 (1986); for analogies with catalysis by complexes, see references therein.
51. Biloen, P., Helle, J. N., Verbeek, H., Dautzenberg, F. M., and Sachtler, W. M. H., *J. Catal.* **63,** 112 (1980).
52. Kern-Tálas, E., Hegedüs, M., Göbölös, S., Szedlacsek, P., and Margitfalvi, J., *in* "Preparation of Catalysts IV" (B. Delmon *et al.*, Eds.), p. 689. Elsevier, Amsterdam/New York.
53. Paál, Z., and Xu, Xian Lun, *Appl. Catal.* **43,** L1 (1988).